



# Rock Magnetism of the Offshore Sediments of Lake Qinghai in the Western China

Peng Zhang<sup>1\*</sup>, Shan Lin<sup>1,2</sup>, Hong Ao<sup>1</sup>, Lijuan Wang<sup>1</sup>, Xiaoyan Sun<sup>1,3</sup> and Zhisheng An<sup>1</sup>

<sup>1</sup> State Key Laboratory of Loess and Quaternary Geology, Institute of Earth Environment, Chinese Academy of Sciences, Xi'an, China, <sup>2</sup> College of Earth Sciences, University of Chinese Academy of Sciences, Beijing, China, <sup>3</sup> College of Urban and Environment Sciences, Shanxi Normal University, Linfen, China

## OPEN ACCESS

### Edited by:

Juan Cruz Larrasoaña,  
Instituto Geológico y Minero de  
España, Spain

### Reviewed by:

Luigi Jovane,  
Instituto Oceanográfico da  
Universidade de São Paulo, Brazil  
Junsheng Nie,  
Lanzhou University, China  
Neli Jordanova,  
National Institute in Geophysics,  
Geodesy and Geography-Bulgarian  
Academy of Science, Bulgaria

### \*Correspondence:

Peng Zhang  
zhangpeng@ieecas.cn

### Specialty section:

This article was submitted to  
Geomagnetism and Paleomagnetism,  
a section of the journal  
Frontiers in Earth Science

**Received:** 04 January 2016

**Accepted:** 13 May 2016

**Published:** 31 May 2016

### Citation:

Zhang P, Lin S, Ao H, Wang L, Sun X  
and An Z (2016) Rock Magnetism of  
the Offshore Sediments of Lake  
Qinghai in the Western China.  
*Front. Earth Sci.* 4:62.  
doi: 10.3389/feart.2016.00062

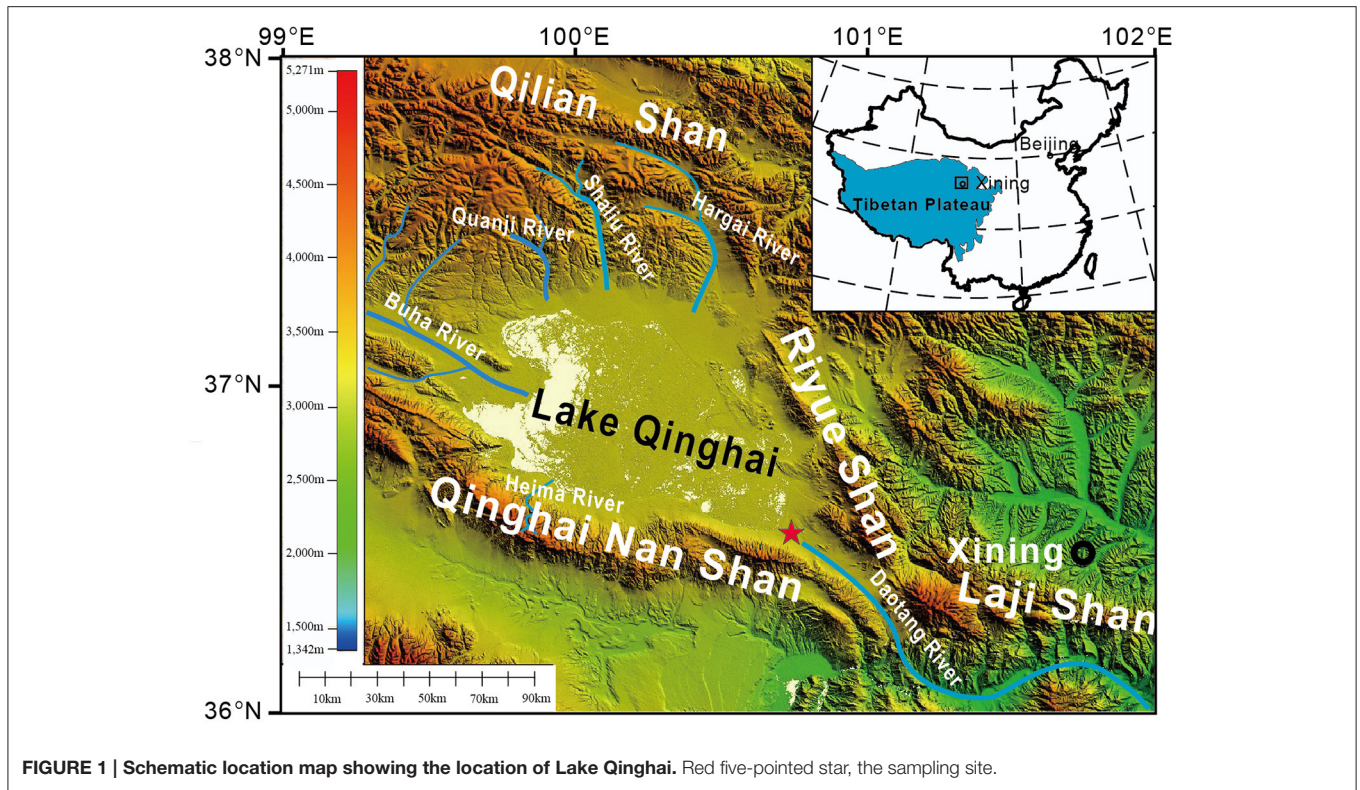
Lake Qinghai is the largest lake in China and situated in an important climate-sensitive zone on the northeastern margin of the Tibetan Plateau, making it an ideal place to study the environmental evolution of the northwest China as well as the interplay between the Asian monsoon and the westerlies in the late Quaternary. In this study, detailed rock magnetic measurements were carried out on the offshore soils of Lake Qinghai. The dry grassland samples have higher magnetic susceptibility than that of the wet grassland samples, which suggests a higher concentration of magnetic minerals in the dry grassland and lower concentration of magnetic minerals in the wet grassland near the lake edge. The high concentration of the superparamagnetic (SP) magnetic minerals related to pedogenesis may also contribute to the high magnetic susceptibility of the dry grassland. The low magnetic susceptibility of the wet grassland may result from the conversion of strongly to weakly magnetic minerals and/or the dissolution of magnetic minerals. In addition, the Hm/(Gt+Hm) value has a positive correlation with the water content, thus can be taken as an effective proxy for the soil moisture.

**Keywords:** Lake Qinghai, rock magnetism, pedogenesis, goethite, hematite

## INTRODUCTION

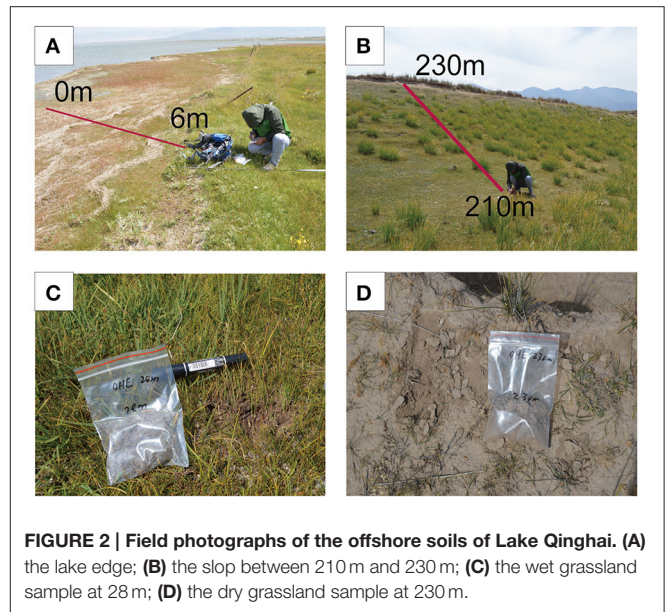
The iron-bearing minerals in rocks and sediments are sensitive to a range of environmental processes, which makes it possible to associate magnetic signals with environmental processes. Environmental magnetism is an interdisciplinary subject involving the application of rock and mineral magnetic techniques to situations in which the transportation, deposition, and transformation of magnetic grains are influenced by environmental processes in the atmosphere, hydrosphere, and lithosphere (Thompson and Oldfield, 1986; Oldfield, 1991; Verosub and Roberts, 1995; Liu et al., 2012). In recent decades, with the rapid development of the techniques for identifying magnetic minerals, environmental magnetism has been employed as an effective tool in the researches of sedimentation processes and environmental evolution recorded in marine and lacustrine sediments, loess-paleosol sequences, and soils (Kämpf and Schwertmann, 1983; Heller and Evans, 1995; Dekkers, 1997; Maher et al., 2002; Evans and Heller, 2003; van der Zee et al., 2003; Deng et al., 2007; Liu et al., 2007; Zhang et al., 2007; Ao et al., 2010).

Lake Qinghai, situated in the sensitive semi-arid zone between the Asian summer monsoon controlled (humid) and the westerlies influenced (arid) areas of Asia, is an ideal site to study the competing influence of two climate system in the late Quaternary (An et al., 2012). Previous



studies have provided valuable information about the climatic changes and their responses to the interplay between the westerlies and the monsoons during the last 36 ka. For example, geochemical and palynological results from sediment cores QH85-14 (Kelts et al., 1989; Lister et al., 1991) and QH2000 (Liu et al., 2003; Shen et al., 2005) suggested a transition towards warm climate in Lake Qinghai at around 14.5 ka. The magnetic susceptibility of the bottom sediments of Lake Qinghai also has been employed as an important climatic proxy in paleoclimate researches (e.g., Wu, 1993; Shen et al., 2001; Zhang et al., 2002). The rock magnetism research was, however, rarely taken in the sediments of Lake Qinghai, which hindered the explanation of environmental magnetism in paleoclimatic studies of Lake Qinghai. The magnetic mineral assemblage in sediments is first influenced by weathering and transport process in the catchment areas. After deposition, it will also be altered by chemical and biogenic processes at the water/sediment interface and during diagenesis (Snowball, 1993; Verosub and Roberts, 1995; Demory et al., 2005). The catchment provides a significant amount of erodible material to the bottom sediment in the lake. As a result, the investigation of modern magnetic minerals in the catchment will enrich our understanding of the migration and alteration processes of magnetic minerals, which is necessary for further application of environmental magnetism in paleoclimatic studies.

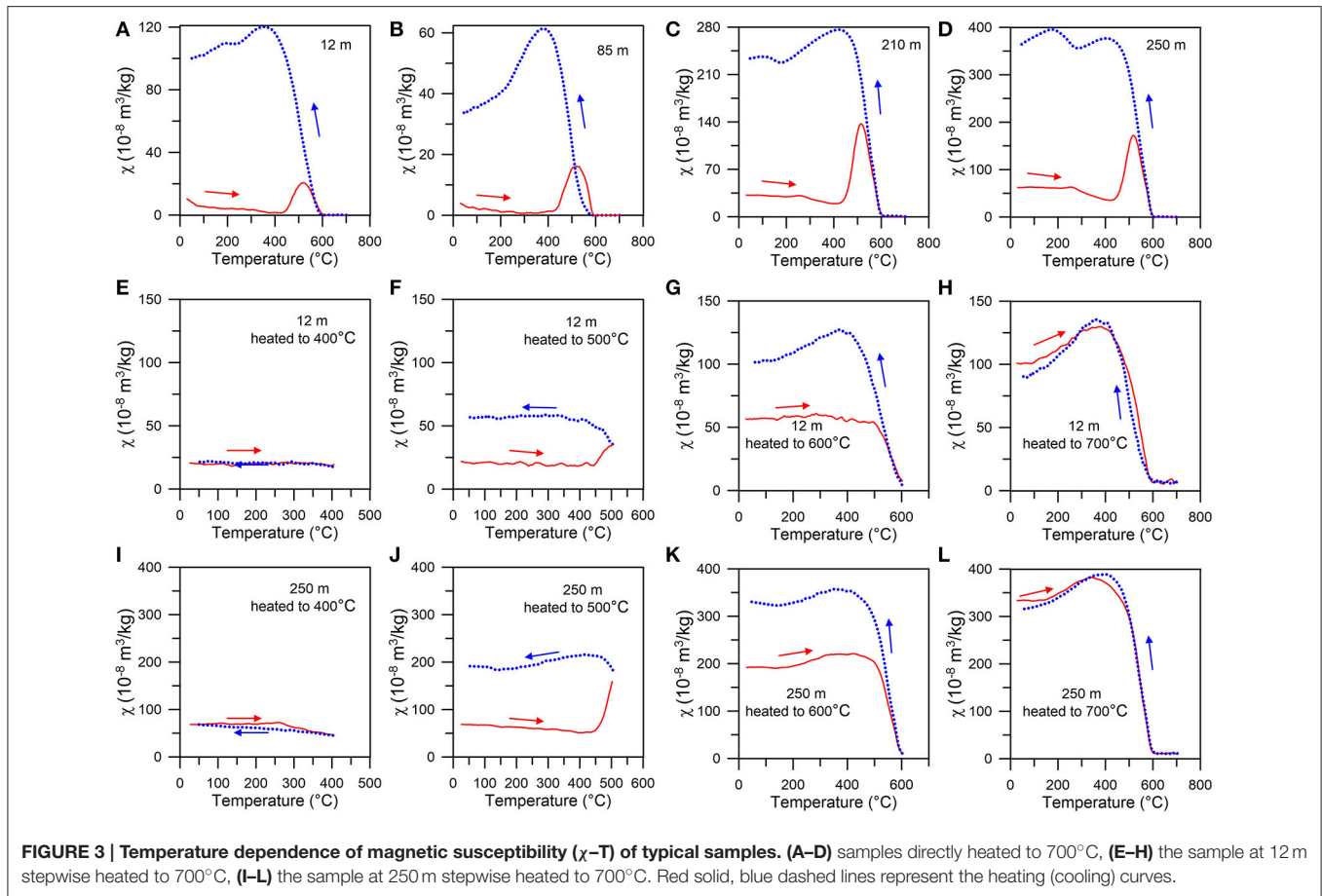
In this study, we carried out detailed rock magnetic measurements on the offshore sediments of Lake Qinghai to improve our understanding of the different magnetic properties related to different sedimentary processes. We further discussed the validity of  $H_m/(Gt+H_m)$  as a proxy for the climate in the offshore sediments.



## GEOLOGICAL SETTING AND SAMPLING

### Geological Setting

Lake Qinghai is located on the northeastern margin of the Tibetan Plateau and west of the Chinese Loess Plateau (Figure 1), with an altitude of 3194 m above current sea level. As the largest saline lake in China, the onset of today's permanent Lake



Qinghai may occur at 11.5 ka, due to a major shift to humid climate throughout the Holocene (Jin et al., 2015). During the last century, the surface of the lake changed from 4980 km<sup>2</sup> to 4260 km<sup>2</sup> in 2006 (Li et al., 2007). The modern lake has a water volume of 71.6 km<sup>3</sup> and a catchment area of about 29,660 km<sup>2</sup>. The lake is currently fed by 5 major rivers, including Buha, Shaliu, Hargai, Quanjia, and Heima Rivers (Figure 1). The primary runoff supply is from the Buha River in the west, which supplies annually ~50% of the total runoff and ~70% of the total sand loading to the lake. From 1951 to 2005, the average annual temperature was ~1.2°C within the catchment of Lake Qinghai. From 1959 to 2011, the annual mean precipitation was 383 mm, about 1/3–1/4 of the annual evaporation (Jin et al., 2011). The lake is frozen from late October to April.

The catchment of Lake Qinghai comprises of predominantly late Paleozoic marine limestone and sandstones, Triassic granites, Mesozoic diorite and granodiorite with minor late Cambrian phyllite and gneiss LIGCAS (1979). Two terraces formed since the last glaciation. The first terrace is mainly wet grassland which is exposed due to the retreat of the lake level thousands of years ago. The soils on the second terrace are developed on the sediments of the Lake Qinghai between 70 and 90 ka (Liu and Lai, 2010), but the sediments have been evolved into soils.

## Field Sampling

We took samples at the end of August when the lake level was the highest. The sampling sites (36°32′37.75″ N, 100°42′38.18″) were located to the southeast of the Lake (Figure 1). Samples were collected along a 330-meter-long transection from the lake edge to the dry grassland (Figure 2). From 0 to 210 m, the ancient offshore alluvial/lacustrine sediments consist of brown-black sapropel with clay or silt (Figures 2A,C). There is a 10-meter-high slope from 210 to 230 m (Figure 2B). The samples of surface soils were collected from 230 to 330 m from the dry gray grassland on the second terrace (Figure 2D). Altogether, 41 samples were collected from the offshore sediments and soils in the southeast of Lake Qinghai.

## METHODOLOGY

### Magnetic Methods

The raw samples were oven dried at 45°C and grinded into powder for magnetic measurements. The low-frequency magnetic susceptibility ( $\chi_{lf}$ ) and high-frequency magnetic susceptibility ( $\chi_{hf}$ ) was measured with a Bartington MS2 meter at a frequency of 470 and 4700 Hz, respectively. Further, the frequency-dependent susceptibility  $\chi_{fd}$  percent was calculated:

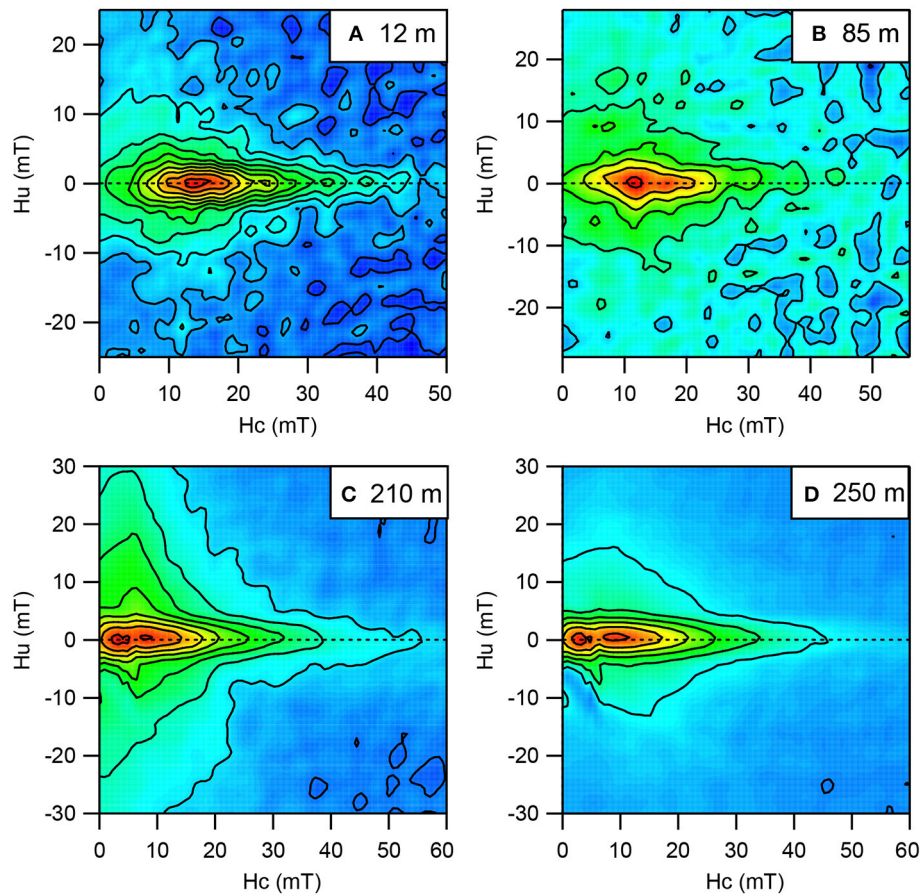


**FIGURE 4 |** FORC diagrams of typical samples. (A) 12 m, (B) 85 m, (C) 210 m, and (D) 250 m.

$\chi_{fd}$  percent =  $(\chi_{lf} - \chi_{hf}) / \chi_{lf} \times 100\%$ . About 300 mg powdered samples were used for measuring temperature-dependent susceptibility ( $\chi$ -T) curves with a MFK1 FA susceptometer equipped with a CS-3 high-temperature furnace (AGICO, Brno, Czech Republic). Measurements were done in an argon atmosphere from room temperature up to 700°C and back to room temperature (heating and cooling rate of  $\sim 6.5^\circ\text{C}/\text{min}$ ). The magnetic field during measurement was 300 A/m (peak-to-peak). The susceptibility of each sample was corrected for the background  $\chi$  (furnace tube correction) using the CUREVAL 8.0 program (AGICO, Brno, Czech Republic). Isothermal remanent magnetization (IRM) acquisition curves were measured with an AGICO JR-6A dual speed spinner magnetometer in a magnetically shielded room (residual field  $< 150$  nT). IRMs were imparted with an impulse magnetizer (ASC, model IM-10-30). IRM acquisition curves consist of 32 field steps with a maximum field of 2.0 T. We define SIRM as IRM acquired at 2000 mT,  $\text{IRM}_{-300}$  as IRM acquired at back-field 300 mT after being saturated at 2000 mT, and S-ratio as  $-\text{IRM}_{-300}/\text{SIRM}$ . The anhysteretic remnant magnetization (ARM) was imparted in a 100 mT alternating field with a superimposed 0.05 mT direct bias field using a D2000T Alternating Field Demagnetizer, and

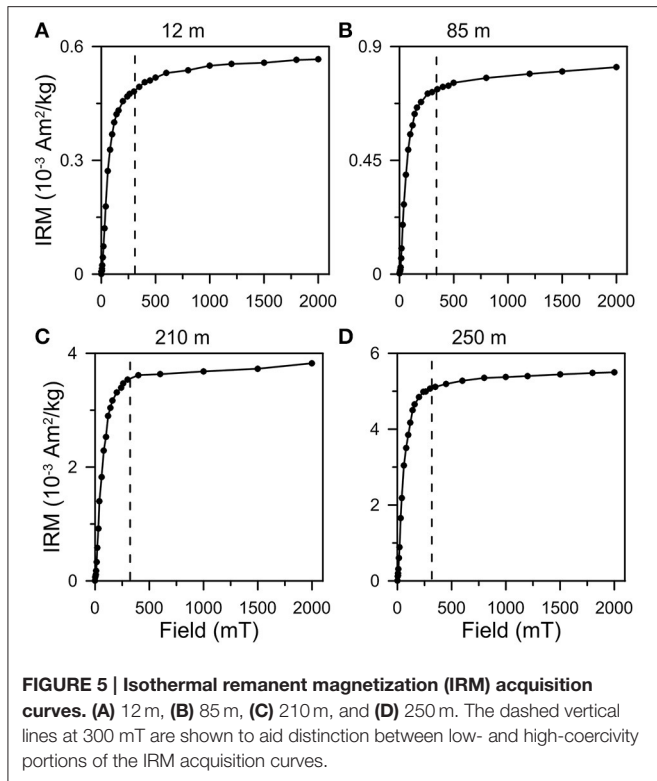
measured with JR-6A dual speed spinner magnetometer. The  $\chi_{\text{ARM}}$  was calculated by dividing the ARM intensity by the DC field strength (0.05 mT).

First-order reversal curve (FORC) diagrams were measured by a Vibrating Sample Magnetometer System (VSM 3900) with a maximum field of 1 T or 1.5 T. 120 FORCs were measured for each sample following the method of Roberts et al. (2000). The FORC diagrams are processed by the FORCinel software (Harrison and Feinberg, 2008) with a smoothing factor (SF) of 7.

The  $\chi$ -T curves were measured at the Institute of Tibet Plateau Research, Chinese Academy of Sciences, CAS, Beijing, and FORC diagrams at the Institute of Geology and Geophysics, CAS, Beijing. The rest of the measurements were performed at the Institute of Earth Environment, CAS, Xi'an.

## Non-magnetic Methods

To obtain the gravimetric water content, powdered samples were oven dried at 105°C for 2 days. We define water content as: the weight of lost water/ the weight of raw sample  $\times 100\%$ . The diffuse reflectance spectroscopy was carried out using Cary 4000



UV-Vis spectrophotometer at a scan rate of 30 nm/min from 350 to 750 nm in 0.5 nm steps and the second derivative was calculated with the Cary UV software.

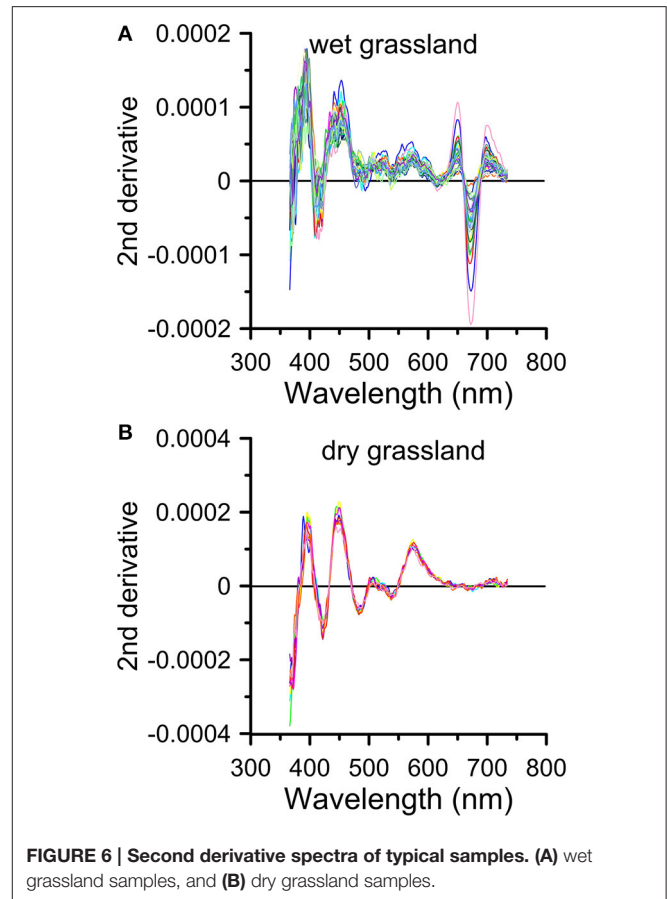
## RESULTS

### $\chi$ -T Curves

The decrease of  $\chi$  between 250 and 450°C in the heating curves of dry grassland samples (**Figures 3C,D**) may result from the inversion of ferrimagnetic maghemite to weakly magnetic hematite (Sun et al., 1995; Deng et al., 2006), suggesting the presence of a small amount of maghemite. The  $\chi$ -T curves of all samples are characterized by a major peak at 450–600°C (**Figures 3A–D**), which is due to the appearance of new strongly magnetic minerals during heating. Step-wise heating of the samples suggests that the peak is related to the thermal transformations during laboratory heating (**Figures 3E–L**). The major drop in magnetic susceptibility at 520–600°C indicates the presence of magnetite in both the samples and the newly formed minerals (**Figure 3**). The transformation of iron oxyhydroxides (e.g., goethite) to a strongly magnetic phase with the presence of organic carbon occurred at 450–600°C according to the stepwise heating curves (Hanesch et al., 2006).

### FORC Diagrams

FORC diagrams can be used to identify and discriminate between the different components in a mixed magnetic mineral assemblage (Roberts et al., 2000, 2014). FORC diagrams of samples at 12 and 85 m show closed contours that diverge along the  $H_c$  axis, suggesting the character of interacting SD



behavior (**Figures 4A,B**). The FORC diagrams of the sample at 210 m show wide vertical distribution along  $H_u$  axis with open contours (**Figure 4C**), which may indicate a PSD behavior. In addition, the low coercivity peak near the origin of the FORC diagram indicates the signals of superparamagnetic (SP) grains. The FORC diagrams of the sample at 250 m show two evident contour peaks of both SD and SP grains (**Figure 4D**), which may imply the presence of both SD and SP grains (Roberts et al., 2000).

### IRM Analyses

All IRM acquisition curves undergo a major increase at low field and the acquired IRM reaches more than 85% of the SIRM at 300 mT (**Figure 5**), suggesting the dominance of low-coercivity magnetic minerals. But the IRM is not totally saturated up to 2.0 T (**Figure 5**), suggesting the presence of low concentration of high-coercivity magnetic minerals (e.g., hematite or goethite).

### DRS Results

The difference in ordinate between the trough and the next peak at a longer wavelength, the band intensity, has been used as a proxy for the true band amplitude (Scheinost et al., 1998). In the second derivative of the reflectance spectrum, the band intensity at 424 nm ( $I_{424}$ ) and 535 nm ( $I_{535}$ ) is proportional to the

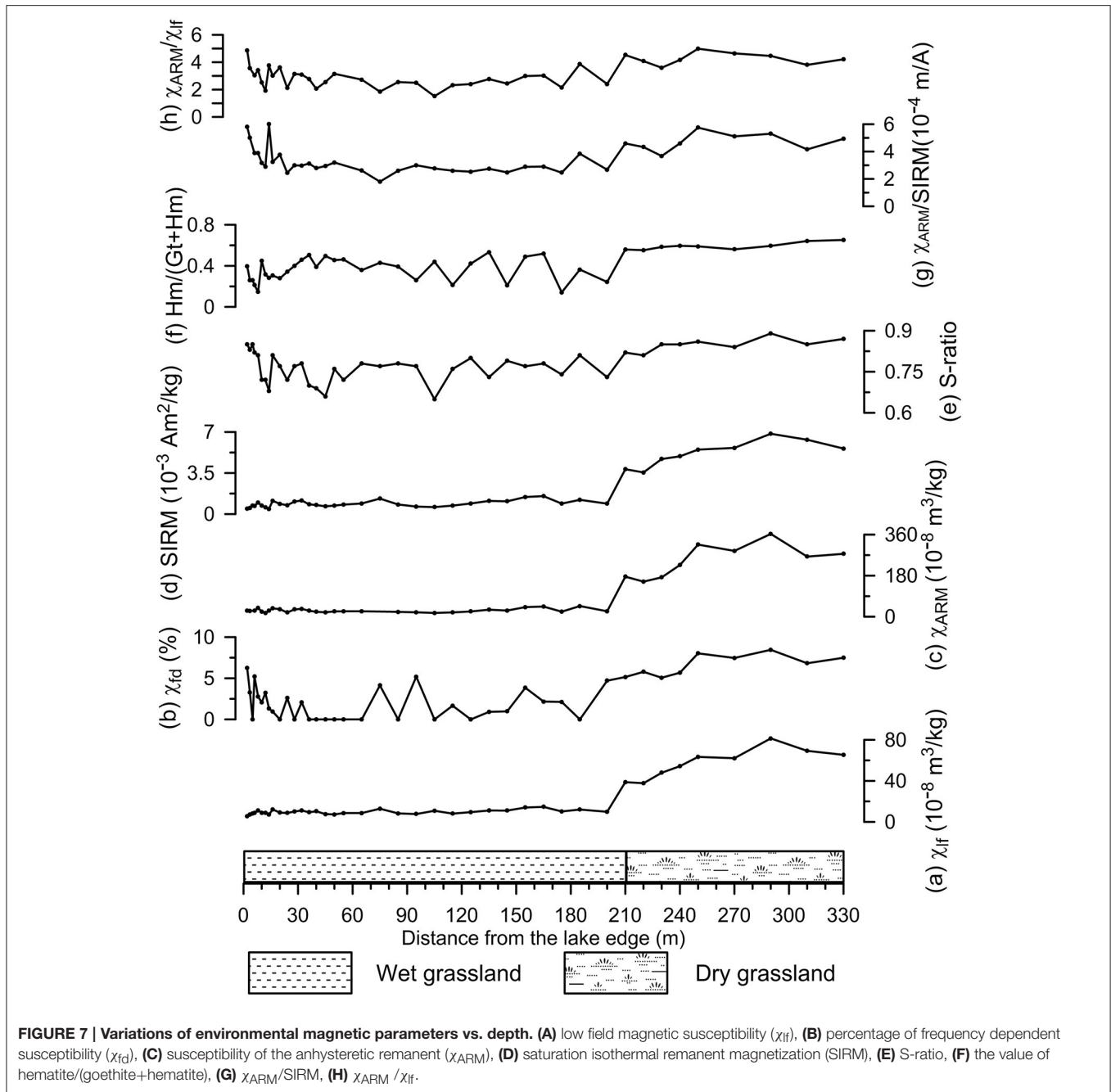


**FIGURE 7 | Variations of environmental magnetic parameters vs. depth. (A)** low field magnetic susceptibility ( $\chi_{lf}$ ), **(B)** percentage of frequency dependent susceptibility ( $\chi_{fd}$ ), **(C)** susceptibility of the anhysteretic remanent ( $\chi_{ARM}$ ), **(D)** saturation isothermal remanent magnetization (SIRM), **(E)** S-ratio, **(F)** the value of hematite/goethite+hematite, **(G)**  $\chi_{ARM}/SIRM$ , **(H)**  $\chi_{ARM}/\chi_{lf}$ .

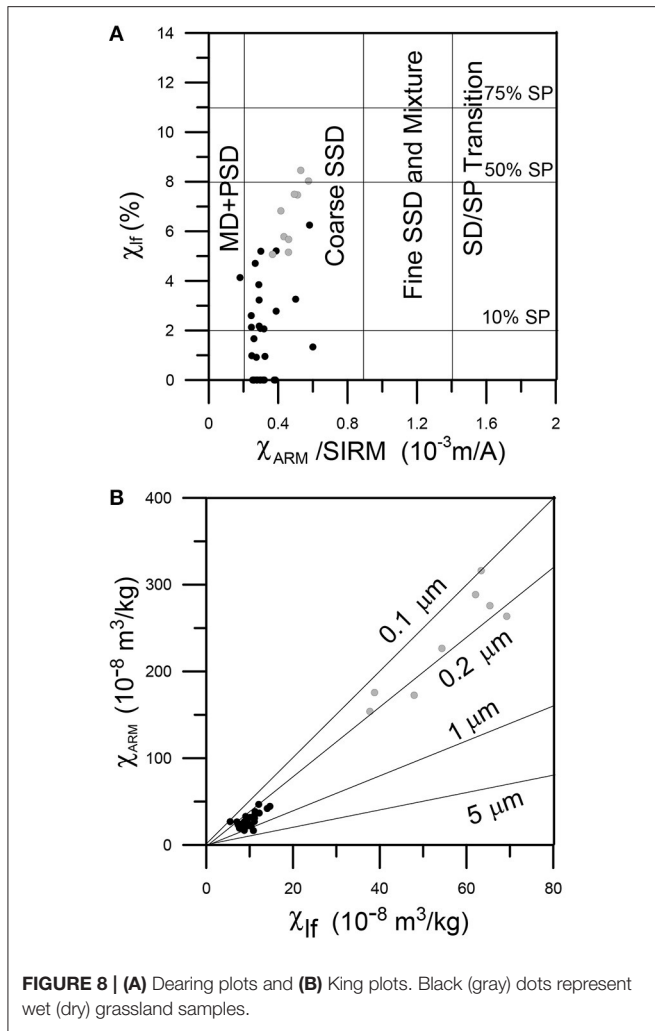
concentration of goethite and hematite, respectively (Scheinost et al., 1998; Torrent et al., 2007). For most samples in this study, the  $I_{425}$  is more evident than  $I_{535}$  (Figure 6). Nonetheless, the band intensity is not the real concentration of the goethite or hematite, because the reflectance can be affected by other admixed minerals (the matrix effect) (Deaton and Balsam, 1991; Ji et al., 2002). The  $I_{535}$  of the wet grassland is not evident compared to that of the dry grassland, which may be related to the low concentration of the hematite in the wet grassland. In this study, we calculated the ratio  $Hm/(Gt+Hm)$  along the

transection following the regression functions of Torrent et al. (2007):

$$Y = -0.133 + 2.871 * X - 1.709 * X^2,$$

Where,  $Y = \text{Hematite} / (\text{Hematite} + \text{Goethite})$ ,  
 $X = I_{535} / (I_{425} + I_{535})$ .

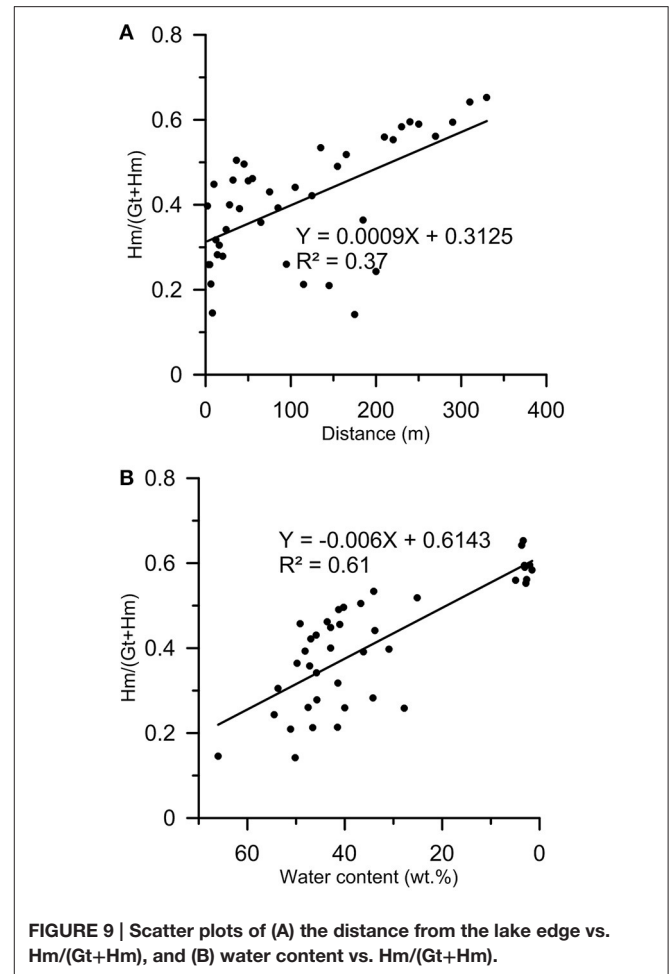
We only calculated the value of Y, which is not the absolute content of hematite or goethite, because the calculation of the citrate-bicarbonate-dithionite (CBD) extractable Fe remains controversial (Torrent et al., 2007; Buggle et al., 2014).



## DISCUSSION

The  $\chi$ -T curves imply the presence of magnetite in both wet and dry grassland, but that of maghemite only in the dry grassland. The high value of  $\chi_{fd}$  also suggests the presence of SP grains in the dry grassland. The FORC diagrams illustrate the dominant SD behavior in the wet grassland and the presence of SP, SD, and PSD grains in the dry grassland. The IRM and S-ratio suggests that the low-coercivity magnetic minerals dominate in all the samples (Figures 5, 7E). Nonetheless, the IRM is not saturated at 2000 mT due to the presence of high-coercivity magnetic minerals (e.g., hematite and goethite). Additionally, the band intensity in the second derivative of the reflectance spectrum also provides evidences for the presence of goethite and hematite in the dry grassland and only goethite in the wet grassland (Figure 6).

When magnetite dominates the magnetic properties of the sediments, the Dearing plot and King plot can be used to estimate the grain size of the ferrimagnets (King et al., 1982; Dearing et al., 1997). Both the wet grassland and dry grassland samples are located in the coarse stable SD (SSD) region (Figure 8A), but the dry grassland samples show more SP contribution. The dry grassland samples are within 0.1–0.2  $\mu\text{m}$  size range while



most of the wet grassland samples within 0.2–1  $\mu\text{m}$  (Figure 8B). Inter-parameter proxies for magnetic grain-size variation, such as  $\chi_{ARM}/\chi_{lf}$  and  $\chi_{ARM}/\text{SIRM}$ , are sensitive to climate (Bloemendal and Liu, 2005). For example,  $\chi_{ARM}/\chi_{lf}$  and  $\chi_{arm}/\text{SIRM}$  of surface soils on the Chinese Loess Plateau are proportional to annual mean temperature and annual mean precipitation (Nie et al., 2014). But in this study, these two values increased from wet grassland to dry grassland (Figures 7G,H), opposite to the results of Nie et al. (2014), which may be due to the different conversion process of magnetic minerals between the surface soils of Chinese Loess Plateau and the offshore sediments of Lake Qinghai.

The  $\chi_{lf}$ ,  $\chi_{fd}$  percent,  $\chi_{ARM}$ , and SIRM show similar trend along the transection from the lake edge to the dry grassland. All the parameters are relatively low in the wet grassland, but increase sharply in the dry grassland (Figures 7A–D). Consequently, we speculate that the wet grassland has lower concentration of total magnetic minerals than the dry grassland. The  $\chi_{lf}$  of wet grassland is usually less than  $15 \times 10^{-8} \text{ m}^3/\text{kg}$ . The value is of the same magnitude as the  $\chi$  of typical lacustrine sediments in northwest China, such as Pliocene and Holocene sediments of Lake Qinghai (Jun and Kelts, 2002; Fu et al., 2015), the Oligocene-Miocene lacustrine sediments in the Xining basin (Fang et al., 2015) and Oligocene lacustrine sediments in the

Lanzhou basin (Zhang et al., 2015). The  $\chi_{lf}$  of dry grassland is usually over  $35 \times 10^{-8} \text{ m}^3/\text{kg}$ , the same as the loess deposited in the Lake Qinghai region (Hunt et al., 1995; Lu et al., 2004; Wang et al., 2015).

The different magnetic properties of the wet and dry grassland may be linked to different conversion process of magnetic minerals, pedogenesis in the dry grassland, and/or the dissolution of magnetic minerals in the wet grassland. Magnetic minerals could be converted to goethite or other weakly magnetic minerals owing to the high water content of wet grassland, but converted to ferrimagnetic minerals in dry grassland, a hypothesis raised by Nie et al. (2016) based on the magnetic properties of red-clay on the Chinese Loess Plateau. However, the different mineral transform route needs detailed study in the future.

The pedogenic fine-grained (SP+SD) maghemite is responsible for the enhanced magnetic susceptibility in the paleosols on the Chinese Loess Plateau (Zhou et al., 1990; Deng et al., 2000; Liu et al., 2007). In this study, the high magnetic susceptibility, the presence of SP and SD grains and maghemite may point to pedogenesis in the dry grassland. Besides, the dissolution of the magnetic minerals in the wet grassland may also contribute to the low magnetic susceptibility. The unusually low  $\chi_{lf}$ ,  $\chi_{ARM}$ , and SIRM compared to the dry grassland soils may be due to the removal of most magnetite particles. What is more, the soils of dry grassland have a much wider magnetic grain-size distribution (SP, SD, and PSD particles), while the soils of wet grassland have a narrow grain-size distribution (SD particles). The several lines of evidence suggest that the pedogenesis and magnetic mineral dissolution are potential causes of different magnetic properties between the wet and dry grassland.

Of a variety of magnetic minerals, the hematite ( $\alpha\text{-Fe}_2\text{O}_3$ ) and goethite ( $\alpha\text{-FeOOH}$ ) which commonly occur in soils and sediments, are especially sensitive to the environmental variation. The transformations from ferrihydrite to hematite and goethite are favored by opposite climate conditions. Hematite is interpreted as being indicative of warm and dry conditions, while goethite indicative of cold and wet conditions (Kämpf and Schwertmann, 1983; Ji et al., 2004). Consequently, the ratio of hematite to goethite (Hm/Gt) or hematite to (goethite+hematite) (Hm/(Gt+Hm)) has been used as a climatic proxy in the paleoclimate studies (Ji et al., 2002; Zhang et al., 2007, 2009; Hao et al., 2009).

In this study, the Hm/(Gt+Hm) value has an indistinctive positive correlation ( $R^2 = 0.37$ , **Figure 9A**) with the distance from the lake edge (**Figure 7F**), which may be due to the abnormal water content of four samples at 115, 145, 175, and 200 m. The  $I_{535}$  of the wet grassland is not evident compared to that of the dry grassland, which may be related to the low concentration

of the hematite in the wet grassland. However, the Hm/(Gt+Hm) value has a much more positive correlation with the water content ( $R^2 = 0.61$ , **Figure 9B**), despite the low concentration of the hematite in the wet grassland. High value of Hm/(Gt+Hm) corresponds to low soil moisture, and vice versa. This suggests that the Hm/(Gt+Hm) value can be taken as an effective proxy for soil moisture, in line with the results from a 600 km E-W transect in south Brazil (Kämpf and Schwertmann, 1983). In paleoclimate studies, the Hm/(Gt+Hm) value (or Hm/Gt) was mostly regarded as an indicator of precipitation (Harris and Mix, 2002; Ji et al., 2004; Zhang et al., 2007). For example, the hematite/goethite (Hm/Gt) ratios are lower in paleosols (formed during wet period) than in loess (formed during dry period) (Ji et al., 2004). Modern process [this study and the results of Kämpf and Schwertmann (1983)] proves the validity for the use of Hm/Gt ratios in the paleoclimate researches.

## CONCLUSIONS

In this study, detailed rock magnetic measurements were carried out in the offshore soils of Lake Qinghai. The results show a higher magnetic susceptibility of dry grassland samples than that of wet grassland, suggesting a higher concentration of magnetic minerals in the dry grassland and lower concentration of magnetic minerals in the wet grassland near the lake edge. The different magnetic properties of the wet and dry grassland may be linked to different conversion process of magnetic minerals, pedogenesis in the dry grassland, and/or the dissolution of magnetic minerals in the wet grassland. Besides, the Hm/(Gt+Hm) value can be taken as an effective proxy for soil moisture.

## AUTHOR CONTRIBUTIONS

PZ, HA, and ZA designed the study and contributed to discussion and interpretation of the results. PZ performed the fieldwork and led the writing of the paper. SL, LW, and XS contributed to the laboratory work and data representation.

## ACKNOWLEDGMENTS

We thank Dawen Zhang and Suzhen Liu for their help in laboratory work. We thank Prof. Weiguo Liu, Huanye Wang, and Yan Yan for their useful suggestions. This study was financially supported by the National Basic Research Program of China (2013CB956402), National Natural Science Foundation of China (41174057, 41290253), and open fund of State Key Laboratory of Loess and Quaternary Geology (SKLLQG1535).

## REFERENCES

- An, Z. S., Colman, S. M., Zhou, W. J., Li, X. Q., Brown, E. T., Jull, A. J. T., et al. (2012). Interplay between the Westerlies and Asian monsoon recorded in Lake Qinghai sediments since 32 ka. *Sci. Rep.* 2:619. doi: 10.1038/srep00619
- Ao, H., Deng, C. L., Dekkers, M. J., and Liu, Q. S. (2010). Magnetic mineral dissolution in Pleistocene fluvio-lacustrine sediments, nihewan basin (North China). *Earth Planet. Sci. Lett.* 292, 191–200. doi: 10.1016/j.epsl.2010.01.035
- Bloemendal, J., and Liu, X. M. (2005). Rock magnetism and geochemistry of two plio-pleistocene chinese loess-palaeosol sequences—implications for

- quantitative palaeoprecipitation reconstruction. *Palaeogeogr. Palaeoclimatol. Palaeoecol.* 226, 149–166. doi: 10.1016/j.palaeo.2005.05.008
- Buggle, B., Hambach, U., Müller, K., Zöller, L., Marković, S. B., and Glaser, B. (2014). Iron mineralogical proxies and Quaternary climate change in SE-European loess–paleosol sequences. *CATENA* 117, 4–22. doi: 10.1016/j.catena.2013.06.012
- Dearing, J., Bird, P., Dann, R., and Benjamin, S. (1997). Secondary ferrimagnetic minerals in Welsh soils: a comparison of mineral magnetic detection methods and implications for mineral formation. *Geophys. J. Int.* 130, 727–736. doi: 10.1111/j.1365-246X.1997.tb01867.x
- Deaton, B. C., and Balsam, W. L. (1991). Visible spectroscopy—a rapid method for determining hematite and goethite concentration in geological materials. *J. Sediment. Res.* 61, 628–632. doi: 10.1306/D4267794-2B26-11D7-8648000102C1865D
- Dekkers, M. J. (1997). Environmental magnetism: an introduction. *Geol. Mijnb.* 76, 163–182. doi: 10.1023/A:1003122305503
- Demory, F., Oberhänsli, H., Nowaczyk, N. R., Gottschalk, M., Wirth, R., and Naumann, R. (2005). Detrital input and early diagenesis in sediments from Lake Baikal revealed by rock magnetism. *Glob. Planet. Change* 46, 145–166. doi: 10.1016/j.gloplacha.2004.11.010
- Deng, C. L., Liu, Q. S., Pan, Y. X., and Zhu, R. X. (2007). Environmental magnetism of chinese loess-paleosol sequences. *Quat. Sci.* 27, 193–209.
- Deng, C. L., Shaw, J., Liu, Q. S., Pan, Y. X., and Zhu, R. X. (2006). Mineral magnetic variation of the Jingbian loess/paleosol sequence in the northern loess plateau of china: implications for quaternary development of asian aridification and cooling. *Earth Planet. Sci. Lett.* 241, 248–259. doi: 10.1016/j.epsl.2005.10.020
- Deng, C. L., Zhu, R. X., Verosub, K. L., Singer, M. J., and Yuan, B. Y. (2000). Paleoclimatic significance of the temperature-dependent susceptibility of holocene loess along a NW-SE transect in the chinese loess plateau. *Geophys. Res. Lett.* 27, 3715–3718. doi: 10.1029/2000GL008462
- Evans, M. E., and Heller, F. (2003). *Environmental Magnetism: Principles and Applications of Enviromagnetics*. Amsterdam: Academic Press.
- Fang, X. M., Zan, J. B., Appel, E., Lu, Y., Song, C. H., Dai, S., et al. (2015). An Eocene–Miocene continuous rock magnetic record from the sediments in the Xining Basin, NW China: indication for Cenozoic persistent drying driven by global cooling and Tibetan Plateau uplift. *Geophys. J. Int.* 201, 78–89. doi: 10.1093/gji/ggv002
- Fu, C. F., Bloemendal, J., Qiang, X. K., Hill, M. J., and An, Z. S. (2015). Occurrence of greigite in the Pliocene sediments of Lake Qinghai, China, and its paleoenvironmental and paleomagnetic implications. *Geochem. Geophys. Geosyst.* 16, 1293–1306. doi: 10.1002/2014GC005677
- Hanesch, M., Stanjek, H., and Petersen, N. (2006). Thermomagnetic measurements of soil iron minerals: the role of organic carbon. *Geophys. J. Int.* 165, 53–61. doi: 10.1111/j.1365-246X.2006.02933.x
- Hao, Q. Z., Oldfield, F., Bloemendal, J., Torrent, J., and Guo, Z. T. (2009). The record of changing hematite and goethite accumulation over the past 22 myr on the chinese loess plateau from magnetic measurements and diffuse reflectance spectroscopy. *J. Geophys. Res. Solid Earth* 114:B12101. doi: 10.1029/2009jb006604
- Harris, S. E., and Mix, A. C. (2002). Climate and tectonic influences on continental erosion of tropical South America, 0–13 Ma. *Geology* 30, 447–450. doi: 10.1130/0091-7613(2002)
- Harrison, R. J., and Feinberg, J. M. (2008). FORCinel: An improved algorithm for calculating first-order reversal curve distributions using locally weighted regression smoothing. *Geochem. Geophys. Geosyst.* 9, Q05016. doi: 10.1029/2008GC001987
- Heller, F., and Evans, M. E. (1995). Loess magnetism. *Rev. Geophys.* 33, 211–240. doi: 10.1029/95RG00579
- Hunt, C. P., Banerjee, S. K., Han, J., Solheid, P. A., Oches, E., Sun, W., et al. (1995). Rock-magnetic proxies of climate change in the loess-paleosol sequences of the western Loess Plateau of China. *Geophys. J. Int.* 123, 232–244. doi: 10.1111/j.1365-246X.1995.tb06672.x
- Ji, J. F., Balsam, W., Chen, J., and Liu, L. W. (2002). Rapid and quantitative measurement of hematite and goethite in the chinese loess-paleosol sequence by diffuse reflectance spectroscopy. *Clays Clay Miner.* 50, 208–216. doi: 10.1346/000986002760832801
- Ji, J. F., Chen, J., Balsam, W., Lu, H. Y., Sun, Y. B., and Xu, H. F. (2004). High resolution hematite/goethite records from Chinese loess sequences for the last glacial-interglacial cycle: rapid climatic response of the East Asian Monsoon to the tropical Pacific. *Geophys. Res. Lett.* 31, L03207. doi: 10.1029/2003gl018975
- Jin, Z. D., An, Z. S., Yu, J. M., Li, F. C., and Zhang, F. (2015). Lake Qinghai sediment geochemistry linked to hydroclimate variability since the last glacial. *Quat. Sci. Rev.* 122, 63–73. doi: 10.1016/j.quascirev.2015.05.015
- Jin, Z. D., You, C. F., Yu, J. M., Wu, L. L., Zhang, F., and Liu, H. C. (2011). Seasonal contributions of catchment weathering and eolian dust to river water chemistry, northeastern tibetan plateau: chemical and Sr isotopic constraints. *J. Geophys. Res. Earth Surface (2003–2012)* 116:F04006. doi: 10.1029/2011JF002002
- Jun, Q. Y., and Kelts, K. R. (2002). Abrupt changes in climatic conditions across the late-glacial/Holocene transition on the NE TIBET-Qinghai Plateau: evidence from Lake Qinghai, China. *J. Paleolimnol.* 28, 195–206. doi: 10.1023/A:1021635715857
- Kämpf, N., and Schwertmann, U. (1983). Goethite and hematite in a climosequence in southern Brazil and their application in classification of kaolinitic soils. *Geoderma* 29, 27–39. doi: 10.1016/0016-7061(83)90028-9
- Kelts, K., Zao, C. K., Lister, G. S., Yu, J. Q., Zhang, G. H., Niessen, F., et al. (1989). Geological fingerprints of climate history: a cooperative study of Qinghai lake, China. *Eclogae Geol. Helv.* 82, 167–182.
- King, J., Banerjee, S. K., Marvin, J., and Özdemir, Ö. (1982). A comparison of different magnetic methods for determining the relative grain size of magnetite in natural materials: some results from lake sediments. *Earth Planet. Sci. Lett.* 59, 404–419. doi: 10.1016/0012-821X(82)90142-X
- Li, X. Y., Xu, H. Y., Sun, Y. L., Zhang, D. S., and Yang, Z. P. (2007). Lake-level change and water balance analysis at Lake Qinghai, west China during recent decades. *Water Resour. Manage* 21, 1505–1516. doi: 10.1007/s11269-006-9096-1
- LIGCAS (Lanzhou Institute of Geology of Chinese Academy of Sciences) (1979). *A Synthetically Investigation Report on Qinghai Lake*. Beijing: Science Press.
- Lister, G. S., Kelts, K., Zao, C. K., Yu, J. Q., and Niessen, F. (1991). Lake Qinghai, China: closed-basin like levels and the oxygen isotope record for ostracoda since the latest Pleistocene. *Palaeogeogr. Palaeoclimatol. Palaeoecol.* 84, 141–162. doi: 10.1016/0031-0182(91)90041-O
- Liu, Q. S., Deng, C. L., Torrent, J., and Zhu, R. X. (2007). Review of recent developments in mineral magnetism of the Chinese loess. *Quat. Sci. Rev.* 26, 368–385. doi: 10.1016/j.quascirev.2006.08.004
- Liu, Q. S., Roberts, A. P., Larrasoaña, J. C., Banerjee, S. K., Guyodo, Y., Tauxe, L., et al. (2012). Environmental magnetism: principles and applications. *Rev. Geophys.* 50, RG4002. doi: 10.1029/2012RG000393
- Liu, X. J., and Lai, Z. P. (2010). Lake level fluctuations in Qinghai Lake in the Qinghai-Tibetan Plateau since the last interglaciation: abrief review and new data. *J. Earth. Environ.* 1, 79–89.
- Liu, X. Q., Shen, J., Wang, S. M., Zhang, E. L., and Cai, Y. F. (2003). A 16 000-year paleoclimatic record derived from authigenetic carbonate of lacustrine sediment in Qinghai Lake. *Geol. J. Chin. Univ.* 9, 38–46.
- Lu, H., Wang, X., Ma, H., Tan, H., Vandenbergh, J., Miao, X., et al. (2004). The Plateau Monsoon variation during the past 130 kyr revealed by loess deposit at northeast Qinghai-Tibet (China). *Global Planet. Change* 41, 207–214. doi: 10.1016/j.gloplacha.2004.01.006
- Maher, B. A., Alekseev, A., and Alekseeva, T. (2002). Variation of soil magnetism across the Russian steppe: its significance for use of soil magnetism as a palaeorainfall proxy. *Quat. Sci. Rev.* 21, 1571–1576. doi: 10.1016/S0277-3791(02)00022-7
- Nie, J., Stevens, T., Song, Y., King, J. W., Zhang, R., Ji, S., et al. (2014). Pacific freshening drives Pliocene cooling and Asian monsoon intensification. *Sci. Rep.* 4:5474. doi: 10.1038/srep05474
- Nie, J. S., Song, Y. G., and King, J. W. (2016). A review of recent advances in red-clay environmental magnetism and paleoclimate history on the Chinese Loess Plateau. *Front. Earth Sci.* 4:27. doi: 10.3389/feart.2016.00027
- Oldfield, F. (1991). Environmental magnetism—A personal perspective. *Quat. Sci. Rev.* 10, 73–85. doi: 10.1016/0277-3791(91)90031-O
- Roberts, A. P., Heslop, D., Zhao, X., and Pike, C. R. (2014). Understanding fine magnetic particle systems through use of first-order reversal curve diagrams. *Rev. Geophys.* 52, 557–602. doi: 10.1002/2014RG000462
- Roberts, A. P., Pike, C. R., and Verosub, K. L. (2000). First-order reversal curve diagrams: a new tool for characterizing the magnetic properties of natural samples. *J. Geophys. Res.* 105, 28461–28475. doi: 10.1029/2000JB900326

- Scheinost, A. C., Chavernas, A., Barron, V., and Torrent, J. (1998). Use and limitations of second-derivative diffuse reflectance spectroscopy in the visible to near-infrared range to identify and quantify Fe oxide minerals in soils. *Clays Clay Miner.* 46, 528–536. doi: 10.1346/CCMN.1998.0460506
- Shen, J., Liu, X. Q., Wang, S. M., and Matsumoto, R. (2005). Palaeoclimatic changes in the Qinghai Lake area during the last 18,000 years. *Quat. Int.* 136, 131–140. doi: 10.1016/j.quaint.2004.11.014
- Shen, J., Zhang, E. L., and Xia, W. L. (2001). Records from lake sediments of the Qinghai Lake to mirror climatic and environmental changes of the past about 1000 years. *Quat. Sci.* 21, 508–513.
- Snowball, I. (1993). Mineral magnetic properties of Holocene lake sediments and soils from the Kårsa valley, Lappland, Sweden, and their relevance to palaeoenvironmental reconstruction. *Terra Nova* 5, 258–270. doi: 10.1111/j.1365-3121.1993.tb00257.x
- Sun, W. W., Banerjee, S. K., and Hunt, C. P. (1995). The role of maghemite in the enhancement of magnetic signal in the Chinese loess-paleosol sequence: An extensive rock magnetic study combined with citrate-bicarbonate-dithionite treatment. *Earth Planet. Sci. Lett.* 133, 493–505. doi: 10.1016/0012-821X(95)00082-N
- Thompson, R., and Oldfield, F. (1986). *Environmental Magnetism*. London: Allen and Unwin.
- Torrent, J., Liu, Q. S., Bloemendal, J., and Barrón, V. (2007). Magnetic enhancement and iron oxides in the upper Luochuan loess-paleosol sequence, Chinese Loess Plateau. *Soil Sci. Soc. Am. J.* 71, 1570–1578. doi: 10.2136/sssaj2006.0328
- van der Zee, C., Roberts, D. R., Rancourt, D. G., and Slomp, C. P. (2003). Nanogoethite is the dominant reactive oxyhydroxide phase in lake and marine sediments. *Geology* 31, 993–996. doi: 10.1130/G19924.1
- Verosub, K. L., and Roberts, A. P. (1995). Environmental magnetism: Past, present, and future. *J. Geophys. Res.* 100, 2175–2192. doi: 10.1029/94JB02713
- Wang, X. Y., Yi, S., Lu, H., Vandenberghe, J., and Han, Z. (2015). Aeolian process and climatic changes in loess records from the northeastern Tibetan Plateau: response to global temperature forcing since 30 ka. *Paleoceanography* 30, 612–620. doi: 10.1002/2014PA002731
- Wu, R. J. (1993). Magnetic susceptibility ( $\chi$ ) and frequency dependent susceptibility ( $\chi_{fd}$ ) of lake sediments and their paleoclimatic implication—The case of recent sediments of Qinghai Lake and Daihai Lake. *J. Lake Sci.* 5, 128–135. doi: 10.18307/1993.0204
- Zhang, E. L., Shen, J., Wang, S. M., Xia, W. L., and Jin, Z. D. (2002). Climate and environment change during the past 900 years in Qinghai Lake. *J. Lake Sci.* 14, 30–38.
- Zhang, P., Ao, H., An, Z. S., and Wang, Q. S. (2015). Rock magnetism properties of Oligocene sediments in the Lanzhou Basin. *Chin. J. Geophys. Chin. Ed.* 58, 2445–2459. doi: 10.6038/cjg20150721
- Zhang, Y. G., Ji, J. F., Balsam, W., Liu, L. W., and Chen, J. (2009). Mid-Pliocene Asian monsoon intensification and the onset of Northern Hemisphere glaciation. *Geology* 37, 599–602. doi: 10.1130/G25670A.1
- Zhang, Y. G., Ji, J. F., Balsam, W. L., Liu, L. W., and Chen, J. (2007). High resolution hematite and goethite records from ODP 1143, South China Sea: Co-evolution of monsoonal precipitation and El Niño over the past 600,000 years. *Earth Planet. Sci. Lett.* 264, 136–150. doi: 10.1016/j.epsl.2007.09.022
- Zhou, L. P., Oldfield, F., Wintle, A. G., Robinson, S. G., and Wang, J. T. (1990). Partly pedogenic origin of magnetic variations in Chinese loess. *Nature* 346, 737–739. doi: 10.1038/346737a0

**Conflict of Interest Statement:** The authors declare that the research was conducted in the absence of any commercial or financial relationships that could be construed as a potential conflict of interest.

Copyright © 2016 Zhang, Lin, Ao, Wang, Sun and An. This is an open-access article distributed under the terms of the Creative Commons Attribution License (CC BY). The use, distribution or reproduction in other forums is permitted, provided the original author(s) or licensor are credited and that the original publication in this journal is cited, in accordance with accepted academic practice. No use, distribution or reproduction is permitted which does not comply with these terms.